

Molecular docking of thiamine reveals similarity in binding properties between the prion protein and other thiamine-binding proteins

Nataraj S. Pagadala · Trent C. Bjorndahl ·
Nikolay Blinov · Andriy Kovalenko · David S. Wishart

Received: 16 May 2013 / Accepted: 21 August 2013 / Published online: 15 October 2013
© Springer-Verlag Berlin Heidelberg 2013

Abstract Prion-induced diseases are a global health concern. The lack of effective therapy and 100 % mortality rates for such diseases have made the prion protein an important target for drug discovery. Previous NMR experimental work revealed that thiamine and its derivatives bind the prion protein in a pocket near the N-terminal loop of helix 1, and conserved intermolecular interactions were noted between thiamine and other thiamine-binding proteins. Furthermore, water-mediated interactions were observed in all of the X-ray crystallographic structures of thiamine-binding proteins, but were not observed in the thiamine–prion NMR study. To better understand the potential role of water in thiamine–prion binding, a docking study was employed using structural X-ray solvent. Before energy minimization, docked thiamine assumed a “V” shape similar to some of the known thiamine-dependent proteins. Following minimization with NMR-derived restraints, the “F” conformation was observed. Our findings confirmed that water is involved in ligand stabilization and phosphate group

interaction. The resulting refined structure of thiamine bound to the prion protein allowed the 4-aminopyrimidine ring of thiamine to π -stack with Tyr150, and facilitated hydrogen bonding between Asp147 and the amino group of 4-aminopyrimidine. Investigation of the π -stacking interaction through mutation of the tyrosine residue further revealed its importance in ligand placement. The resulting refined structure is in good agreement with previous experimental restraints, and is consistent with the pharmacophore model of thiamine-binding proteins.

Keywords Prion protein · Thiamine · Water interaction · Pi stacking

Introduction

Transmissible spongiform encephalopathies (TSEs) or prion diseases are fatal neurodegenerative disorders that are characterized by the accumulation of a protease-resistant form of the prion protein (Fig. 1) in the brain [1, 2]. The disease arises when the normal cellular helix-rich protein (PrP^C) is converted into an abnormally folded, disease-related isoform (PrP^{Sc}) that is rich in β -sheet structure. TSEs are invariably fatal, as there is currently no effective therapy or vaccine for them. Consequently, numerous studies have been directed toward the development of therapeutics to prevent the conversion of PrP^C to PrP^{Sc}. However, these therapeutic developmental efforts are being undertaken despite the lack of a detailed understanding of the cellular mechanism of prion propagation. While many ligand therapeutic studies have been directed toward the prion protein, none have proven successful in animal studies. One proposed mechanism for therapeutic intervention involves the direct stabilization of the prion protein, which would prevent the initial unfolding event and halt β -isoform replication. In order to facilitate the development of such ligands in silico, a

Electronic supplementary material The online version of this article (doi:10.1007/s00894-013-1979-5) contains supplementary material, which is available to authorized users.

N. S. Pagadala (✉)
Department of Electrical and Computer Engineering, University of
Alberta, W4-021 ECERF Building, Edmonton, Alberta,
Canada T6G 2 V4
e-mail: nattu251@rediffmail.com

T. C. Bjorndahl · D. S. Wishart
Departments of Biological Sciences and Computing Science,
University of Alberta, Edmonton, Alberta, Canada T6G 2E8

N. Blinov · A. Kovalenko
Department of Mechanical Engineering, University of Alberta,
Edmonton, Alberta T6G 2G8, Canada

N. Blinov · A. Kovalenko · D. S. Wishart
National Institute for Nanotechnology, 11421 Saskatchewan Drive,
Edmonton, Alberta, Canada T6G 2M9

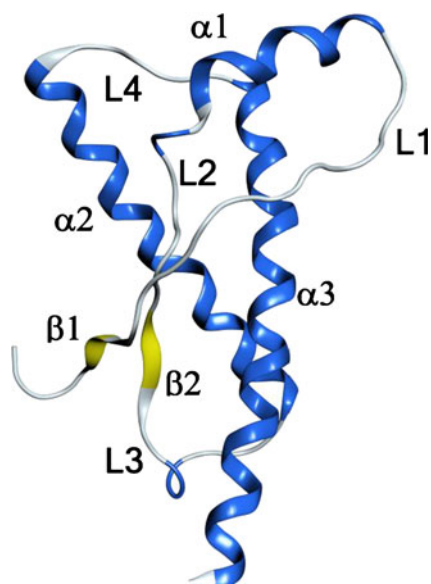


Fig. 1 Ribbon representation of the native, nonpathogenic form of the prion protein. Alpha (α) helices are colored *blue*, beta (β) sheets are colored *yellow*, and loop (L) regions are colored *gray*

good working model of the protein is required. Furthermore, one which could be validated experimentally would be ideal. However, to date, only one such structural study of the prion protein with a bound ligand has been reported [3]. Interestingly, the study found that thiamine and its phosphorylated derivatives exhibited consistent binding constants of $\sim 60 \mu\text{M}$ for various mammalian strains of the prion protein (hamster, mouse, and human). The vast majority of ^{15}N -HSQC perturbed signals localized the binding site to residues Met138, Met139, His140, Gly142, and Tyr150 (see Fig. S1 of the “Electronic supplementary material,” ESM). While these findings were novel and clearly identified a previously undiscovered interaction site, they were unable to explain why various phosphorylated forms of thiamine had no effect on the prion-binding affinities. Furthermore, the NMR study was unable to examine the potential mediation of intermolecular interactions by water, which is observed in all the other structures of thiamine-binding proteins that have been solved via X-ray crystallography. These thiamine-binding proteins include mouse pyrophosphokinase (MPPK), cancer-associated *Mycoplasma hyorhinis* protein (MHP37), pyruvate dehydrogenase complex (PDH), and human transketolase (HTK). Unfortunately, this isoform of the native prion protein does not yield well-diffracting crystals that are compatible with high-resolution X-ray crystallography. Thus, to overcome these shortcomings with both NMR and X-ray crystallography, we developed a robust *in silico* docking protocol to further explore the molecular details of water and thiamine interactions. In doing so, we have developed a model of the prion protein that can provide the starting point for *in silico* protein–ligand studies of targeted “hotspot” regions for prion protein stabilization.

Briefly, we first developed a robust computational protocol that correctly bound thiamine and its derivatives to all known thiamine-binding proteins with high precision. This protocol was then employed for the prion protein (i.e., Syrian hamster prion or ShPrP), both with and without X-ray solvent, which provided alternate docking confirmations. Initially, thiamine adopted the higher-energy “V” conformation, defined by torsion angles ϕT and ϕP of $\pm 90^\circ$ and $\pm 90^\circ$, respectively; here, ϕT is the angle $\text{C}(5')\text{--C}(3,5')\text{--N}(3)\text{--C}(2)$ and ϕP is the angle $\text{N}(3)\text{--C}(3,5)\text{--C}(5')\text{--C}(4')$ (Fig. 2). On the other hand, the alternate, lower-energy, “F” conformation (ϕT and ϕP angles of 0° and $\pm 90^\circ$, respectively) for thiamine was adopted following minimization using NMR-derived restraints. This docking pose is consistent with those seen for other thiamine-binding proteins (MPPK, PDH, and MHP37). In the presence of water, new mechanistic insights were revealed that indicate the conserved involvement of water in the stabilization of thiamine and also in the mediation of interactions with the phosphorylated derivatives, thus negating direct interactions of the phosphate groups with the ShPrP. Such water-mediated interactions would account for the consistent binding constants observed between various phosphorylated forms of thiamine and various mammalian prion strains. The docked F conformer for thiamine bound to the prion protein was in better agreement with NMR restraints than the V conformation was. Given the success of these results, the method presented here is now being used to dock a variety of novel anti-prion compounds with predicted hotspots associated with prion conversion [4, 5]. The docking protocol and its results are described in more detail in the following sections.

Materials and methods

Protein model selection and refinement

MOE 2012.10 (Chemical Computing Group, Montreal, Canada) was used for our *in silico* docking studies. X-ray models of the known thiamine binding proteins—mouse thiamine pyrophosphokinase (MPPK: 2 F17.pdb) [6], cancer-associated *Mycoplasma hyorhinis* protein (MHP37: 3E78.pdb) [7], *E. coli* pyruvate dehydrogenase complex (PDH: 3LQ4.pdb) [8], and human transketolase (HTK: 3OOY.pdb)—were used as is. In order to identify a suitable prion (PrP) structural model for docking, the NMR structures from the Syrian hamster prion protein, ShPrP (1B10.pdb), were superposed and grouped into four different clusters using the first model as a template. One representative model (models 1, 6, 10, and 17 of the original NMR ensemble) was chosen from each cluster. Hydrogen atoms were added, and the structures were further minimized with the CHARMM27 force field [9] using the generalized Born implicit solvent representation [2] until the energy gradient was less than $0.05 \text{ kcal/mol}^{-1}$ [10]. Pairwise alignment of

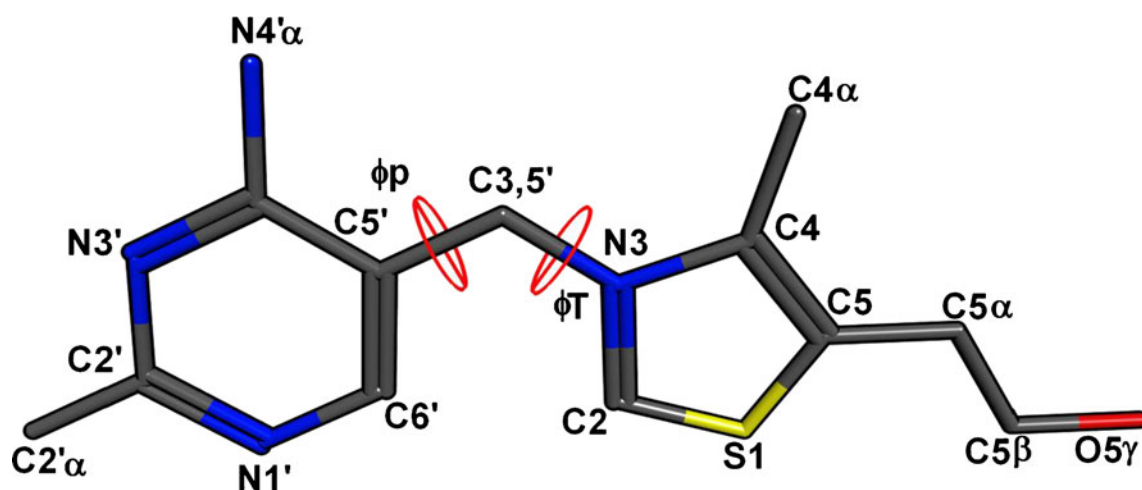


Fig. 2 Molecular structure of thiamine, along with the atom labels used in this study

each model with the average structure revealed that model 17 had the smallest RMSD (0.5 Å), so this model was then used for all subsequent docking studies in the structured solvent. To account for a possible role of bound water molecules in ligand binding, the 105 water coordinates from the X-ray structure of the human prion protein, HuPrP (3HAK.pdb), were transferred to our representative model and energy minimized. The RMSD between the α -carbons of HuPrP and shPrP is 2.7 Å. The same force field and energy minimization protocol as described above was used to confirm proper solvent layer placement and resolve any van der Waal violations.

Thiamine model generation

Ligand templates were constructed and optimized with all hydrogens included using MOE software (Chemical Computing Group) with default parameters and the TAFF force field [11] as well as the implicit generalized Born solvation model, until the energy gradient was less than 1×10^{-5} kcal/mol⁻¹.

Binding site prediction

MOE's alpha site finder was used to identify potential ligand-binding pockets on the protein. In total, four regions of the protein were identified as potential pockets. The three-dimensional coordinates of the receptor atoms were predicted using a modified Delaunay triangulation protocol. Four receptor points for each site without internal atoms were identified and alpha spheres were generated according to the default MOE protocol. More specifically, small alpha spheres in the locations of tight atomic packing were retained and classified into hydrophilic and hydrophobic spheres. Hydrophilic spheres that were not near hydrophobic spheres were eliminated, and the remaining spheres were clustered using the single linkage clustering algorithm to produce the alpha site.

The parameters used employed a probe radius of 1.4 Å for hydrophilic and hydrogen-bonding atoms, a probe radius of 1.8 Å for hydrophobic atoms, 3 Å for isolated donor or acceptor separation, 2.5 Å separation for two individual clusters of alpha spheres to combine to form one cluster, and a minimum of 3 Å for the radii of alpha spheres that comprise a suitable receptor site.

Ligand placement

To perform *in silico* docking of thiamine onto the target proteins, we employed the ligand placement method in MOE called "Alpha PMI" to bias the conformational search of the ligand to meaningful trials. In all cases, the London ΔG method was used for scoring, and the TAFF force field [11] was used for energy minimization. The binding-site side chains were constrained using a force constant of 1.0 kcal/mol⁻¹ Å².

Conformational search

Rotamer generation for Tyr150 (numbering for the Syrian hamster prion protein) was done using the rotamer explorer module in MOE2012.10. Those with χ_1 and χ_2 angles of Tyr150 that could accommodate π -stacking with the 4'-aminopyrimidine of thiamine were selected and used for the preliminary focused docking studies. Subsequent blind docking studies, however, were performed with flexible ligand and side chains. The default MOE docking protocol was used to search the binding conformation space. This protocol allows the ligand to search six rotational, translational, and any number of torsional degrees of freedom during the docking run. The cut-off for the reaction model's dielectric function was between 8 and 10 Å, and the pocket radius was set to 6.0 Å. Ligands protruding out of the docking box were

excluded. The most favorable binding orientations were recognized by matching the ligand template points to the corresponding binding-site alpha spheres. The protein model generated from the favorable rotamer selection was termed “protein model I.” Further energy minimization of this model using the experimental NMR restraints was also performed to generate a second model from directed docking studies; this model was termed “protein model II.”

Scoring and selection

The final docking poses were ranked according to the interaction energies (U_{total} in kcal/mol⁻¹) as the sum of the electrostatic and van der Waals energies and the flexibility of the ligand itself using the London ΔG scoring function. Solvation energies were calculated using the Poisson–Boltzmann equation. The 6–12 Lennard–Jones potential was used for the van der Waal parameter, and the dielectric constant was set to 4 for the Coulombic electrostatic force.

Results

Native docking of thiamine-binding proteins

To evaluate the accuracy of our binding pocket prediction and ligand docking protocol, the following thiamine-dependent enzymes were used as positive controls: MPPK, MHP37, PDH, and HTK. The top-ranking predicted binding sites for these four enzymes agreed very well with their observed experimental X-ray structures (see Fig. S2 of the ESM). The selection of these proteins was based not only on the fact they all bound thiamine but also on the fact that they interacted with conformational diversity of the ligand itself. The thiamine analogs were re-docked with their corresponding proteins in the presence and absence of structural water and counterions for comparison. Analysis of the docked ligands in the presence of crystallographic water and ions indicated π -stacking of thiamine’s 4'-aminopyrimidine ring with the indole group of Trp222 in MPPK, Trp314 in mhp37, and the phenyl groups of Phe602 in PDH and Phe392 in HTK. Analysis of the angles ϕ_T and ϕ_P for thiamine docked in the aforementioned proteins revealed an F conformation for the MPPK (−9.4 and −76) and MHP37 (−24.8 and 94.2) proteins and a V conformation for the PDH (101.9 and −67.5) and HTK (95.4 and −61.5) proteins. While the heavy atom RMSD of the docked conformation compared well with the experimental conformation in the absence of water (2.0, 2.5, 2.4, and 2.7 Å for PPK, MPH37, PDH, and HTK, respectively), they were reduced to about 1.3 Å in the presence of water. In particular, the RMSDs between the predicted and experimental conformations were 1.2, 1.4, 2.6, and 1.2 Å for PPK, MPH37, PDH, and HTK, respectively. Note that the larger

RMSD observed for thiamine diphosphate docked to PDH is largely a consequence of the phosphate moiety and not the core of the thiamine ligand. The core thiamine structure superposed with an all-atom RMSD of 1.2 Å. In all of these thiamine-binding proteins, water molecules mediated hydrogen bonds between the phosphate groups and charged amino acid side chains, and π -stacking was observed between thiamine’s pyrimidine ring and a conserved aromatic residue (see Fig. S3 of the ESM).

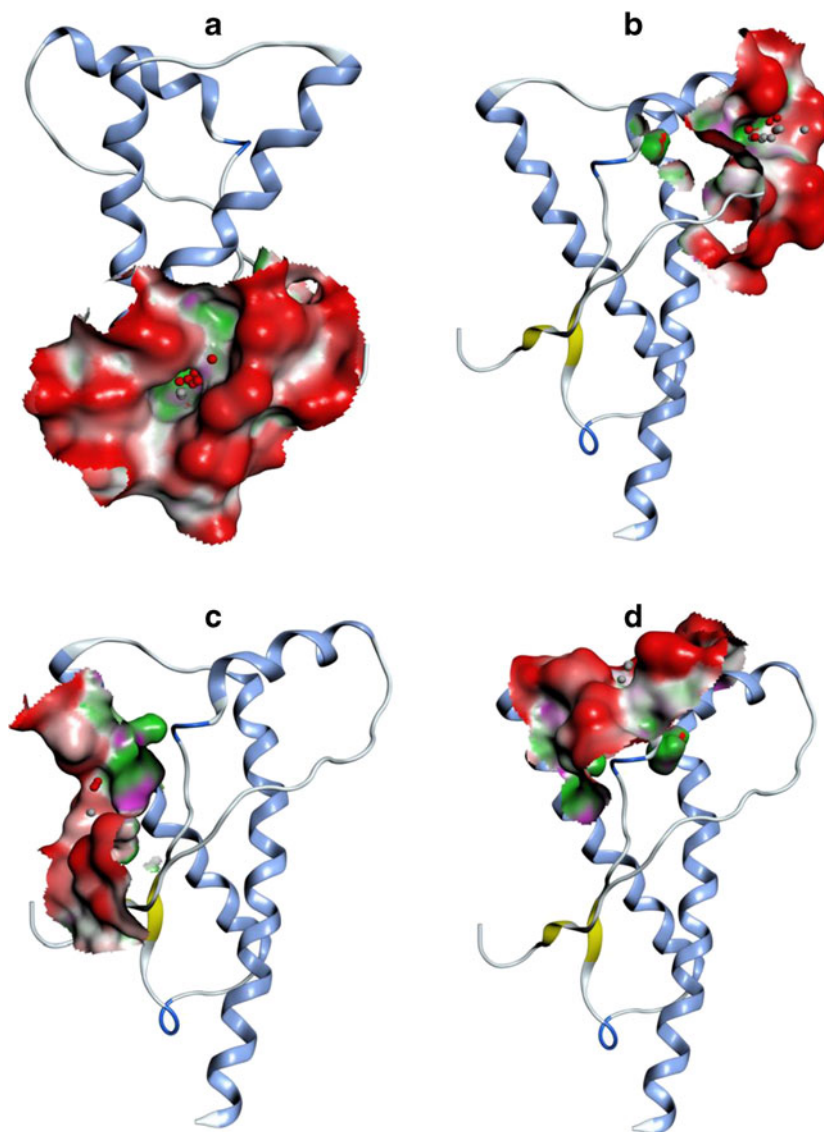
Binding pocket prediction and model selection of ShPrP

As noted earlier, superposition of the 25 NMR models of ShPrP (1B10.pdb) revealed four distinct structural groups based on hierarchical clustering. NMR models #1 and #8 fell under cluster I; models #2, #5, and #6 fell under cluster II; models #10, #12 and #13 fell under cluster III, and the rest fell under cluster IV. Finally, models #1, #6, #10, and #17 were chosen for further docking studies as representative models for each respective cluster based on their extreme pairwise RMSDs relative to each other. For all 25 NMR structures, 13 binding pockets were predicted at pH 7. Four pockets (A–D) were considered major and nine pockets were considered minor based on their number of hydrophobic residues (Fig. 3). Pocket A is part of the “rigid loop” region comprising residues NNQNNF located between beta 2 and helix 2 [4]. Pocket B is the thiamine-binding region located between helix 1 and loop 1 [3], while pocket C is located between helix 2 and loop 2 and is known to bind the anti-prion compound known as GN8 [5]. Finally, pocket D is located between helices 2 and 3 and includes loop 4, which is considered a hotspot for anti-prion compound development [5]. Our preliminary blind docking studies of thiamine and its derivatives against the representative models indicated that these ligands primarily interact with pockets A and C (Fig. 4). Interestingly, three of the four mentioned binding pockets have been confirmed experimentally. Furthermore, SAR studies of the GN8 ligands that target pocket C have also validated the principle of protein stabilization. These findings suggest that the remaining three pockets could also be explored for their potential protein-stabilization effects. While this finding is interesting and worthy of future investigation, our primary interest was in improving the bound thiamine conformer and investigating the role of water in binding, in the hope of developing a robust model to pursue such studies. Thus, because model 17 was shown to dock thiamine favorably in pocket B, it was chosen as the representative structure for follow-up docking studies.

Tyr150 rotamer analysis

Preliminary focused docking of thiamine into pocket B of model 17 (1B10.pdb) was also carried out with relaxed protein

Fig. 3a–d Results obtained from MOE's site finder algorithm. The top four binding pockets (A–D) for the ShPrP, ranked based on the number of hydrophobic residues, are shown. The solvent-accessible surfaces are colored *red*, *gray*, and *green* (the colors represent different levels of hydrophobicity, with red being the least and green the most hydrophobic). Hydrophilic and hydrophobic contributions of the binding pockets are represented by *red* and *white alpha spheres*, respectively



side chains, which allowed π -stacking of thiamine's 4'-aminopyrimidine ring upon rearrangement of the angles χ_1 and χ_2 in Tyr150 (pre: χ_1 and χ_2 : 152.7° and 53° ; post: χ_1 and χ_2 : -149.1° and 103.6°). However, thiamine was still not able to adopt the F conformation that better satisfied experimental restraints [3]. Further, blind docking studies of thiamine were also conducted against an energy-minimized shPrP model (1B10.pdb:17), with native Tyr150 χ_1 and χ_2 angles of 152.7° and 53° and reoriented Tyr150 χ_1 and χ_2 angles of -172° and 81° generated from a rotamer analysis, which allowed for π -stacking. These docking results reiterated the results of the previous binding-site prediction studies, which indicated that thiamine preferentially docks in pocket D rather than pocket B. Thus, a simple rotamer reorientation of Tyr150 was insufficient to correctly identify pocket B and dock thiamine to the shPrP in a blind docking study.

The docked conformation statistics for model #17 are shown in Table 1.

Importance of water

The significance of water-mediated stabilization has previously been discussed in the context of other thiamine-binding proteins (MPPK, MHP37, PDH, and HTK). To evaluate additional roles that water could play in the docking of thiamine to ShPrP, the structured water from the human PrP protein (HuPrP: 3HAK.pdb) was superposed onto ShPrP (1B10:17). The docking studies for the NMR structure (1B10:17) and the energy-minimized ShPrP model in the presence of structural water resulted in the majority of the phosphorylated forms of thiamine being preferentially bound to pockets B and D (Fig. 5a, b). Only about 25 % of the possible conformations

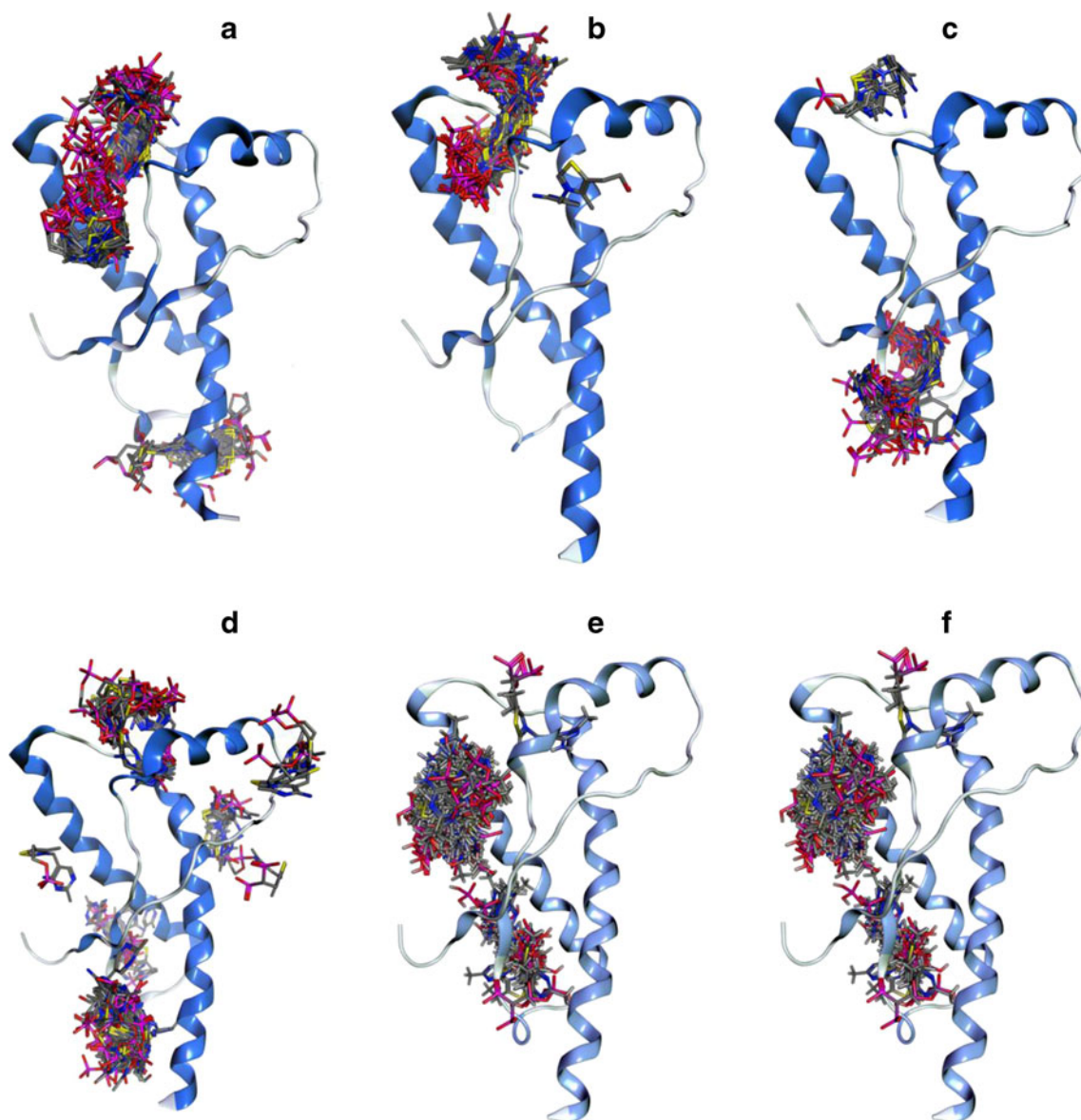


Fig. 4a–f Blind docking results for the phosphorylated forms of thiamine in the absence of water: 1B10:1 (**a**), 1B10:6 (**b**), 1B10:10 (**c**), 1B10:17 (**d**), energy-minimized 1B10:17 (**e**), and energy-minimized

1B10:17-Y150 rotamer (**f**). Ligand clusters are shown as *stick models* and the protein is represented as a *ribbon*. Docked conformations cluster in the previously identified binding pockets (see Fig. 3)

occupied pocket B with the native Tyr150 rotamer of model 17. However, upon using the new side-chain orientation of Tyr150, the majority of the ligand conformations occupied pocket B, with pocket C accommodating a small percentage of the remaining conformers (Fig. 5c). This protein conformation with the new side-chain orientation of Tyr150 was named “protein I.” Further energy minimization of the protein was performed using the NMR restraints from PDB file 1LH8, which was named “protein II,” and used exclusively for additional blind docking studies in structured solvent without restraints. Interestingly, all of the docking results using “protein II” converged to pocket B (Table 2) (Fig. 5d). The presence of water molecules in the docking study appears to be critical for reproducing

the experimental docked conformation of thiamine to ShPrP. However, even with the required rotamer manipulation, energy minimization, and flexible docking, thiamine did not dock into the binding site in 25 % of our docking attempts. With additional binding-site manipulation through rotamer screening and restraint refinement, all of the docking results converged.

The V versus the F conformation

Most of the structures generated from the blind docking study of protein I in the presence of structural solvent had thiamine assuming the V conformation in which the C4–NH₂ of the pyrimidine ring approaches the C2–H of the thiazolium. Thus,

Table 1 Statistics for thiamine derivatives docked in the absence of water

Ligand	Pocket A	Pocket B	Pocket C	Pocket D
Model 17 (native)				
Thiamine				25
TMP	2	2	4	18
TDP	2		1	21
TPP	2			25
Energy-minimized model 17 Tyr150 rotamer (χ_1 and χ_2 : -172° and 81°)				
Thiamine	1			25
TMP	10			18
TDP	4		1	21
TPP	3			25

the aromatic rings sit in a *cis* conformation with respect to each other. In these docked conformations, the 4'-aminopyridine

ring sits orthogonal to the aromatic ring of Tyr150, with the amino group oriented into the solvent. The ring and amino group make electrostatic contact with the side chain of Asp147, and the OH and phosphate groups interact with the amide nitrogen of Gly142. The terminal phosphate groups of TMP, TDP, and TPP form hydrogen bonds with the protein's solvation layer. However, the measured NOE distance violations (Table 3) clearly discredit the validity of this docked conformation. NOE restraint minimization of the V conformer allowed the ShPrP to undergo structural changes that orient these thiamine derivatives closer to an F conformation with ϕ_T and $\phi_P \sim 50^\circ$, which compares favorably to the previously reported values: $\phi_T = 3.5^\circ$ and $\phi_P = 86.4^\circ$. Re-docking these ligands with this protein structure (II) allowed the 4'-aminopyrimidine ring to π -stack with Tyr150. In all of these conformations, the 4'-aminopyrimidine ring and the thiazole groups were located within 1 Å of the NMR distance limits shown in Table 4. The N4' atom of thiamine hydrogen-bonds

Fig. 5a–d Docking of thiamine into the four predicted binding pockets (i.e., directed docking). Clusters of thiamine in the presence of water for the ShPrP NMR model (1B10:17) (**a**), for the energy-minimized structure (**b**), for the energy-minimized structure with the π -stacking accommodating rotamer of Tyr150 (**c**), and for the restraint-minimized structure with the π -stacking accommodating rotamer of Tyr150 (**d**)

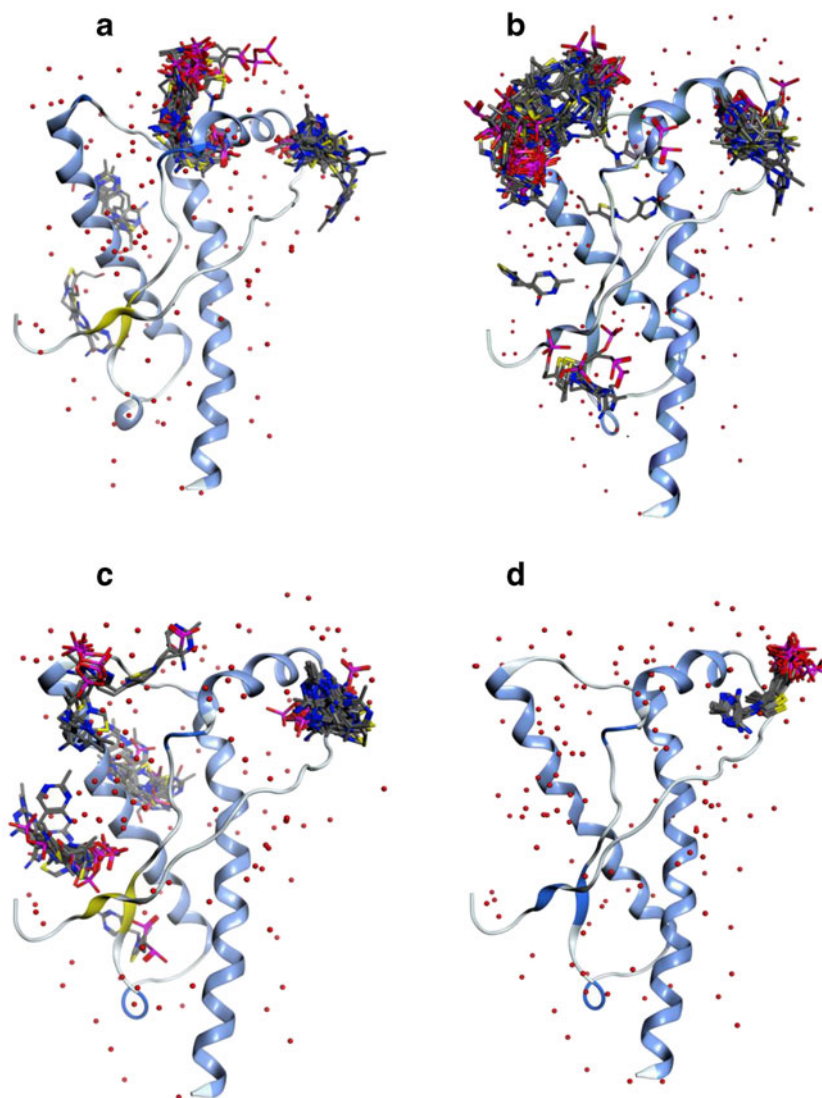


Table 2 Statistics for thiamine derivatives docked in the presence of water

Ligand	Pocket A	Pocket B	Pocket C	Pocket D
Model 17 (native)				
Thiamine		10		15
TMP	2	-		28
TDP	4	2		22
TPP		-		23
Energy-minimized model 17				
Thiamine	3			14
TMP	3	10		9
TDP	1	2		11
TPP		-		28
Energy-minimized model 17 Tyr150 rotamer (χ_1 and χ_2 : -172° and 81°)				
Thiamine		20	2	5
TMP		20	2	5
TDP		20	2	5
TPP		20	2	5

with Asp147 and forms a *trans* conformation with respect to the C2 carbon, thus forming an F conformation (Table 5). A water molecule bridges the interactions between the side chains of Arg151 and the amino group of thiamine's pyrimidine ring (Fig. 6). In addition, thiamine's terminal phosphate groups are involved in water-mediated hydrogen bonding with solvent molecules in the vicinity of the binding pocket.

In silico mutational analysis

In silico mutation of Tyr150 to phenylalanine did not affect the binding orientation of thiamine's 4'-aminopyrimidine ring. However, all other mutations resulted in docked structures with the amino group of the 4'-aminopyrimidine facing towards the protein's interior and the methyl group facing its exterior when Tyr150 was mutated to Ala, Glu, Leu, and Trp. The orientation of the 4'-aminopyrimidine ring did not differ significantly for the Tyr150Leu and Tyr150Trp mutants, in contrast to the orientations formed by the Tyr150Glu and Tyr150Ala mutants. Thus, neither Trp nor Leu could fully replace Tyr150, but both were better substitutes for Tyr150 than Ala or Glu. This suggests that hydrophobic interactions

play an important role in the proper positioning of thiamine into pocket B, and that aromatic residues aid in stabilizing these molecules through π -stacking. However, tryptophan's bulkiness and/or the hydrophobicity of leucine and tryptophan hindered the proper placement of thiamine in the small binding cavity.

Discussion

In many biological processes, ligand–protein interactions are mediated by water. In this study, the implementation of structural solvent docking not only allowed the correct binding site to be identified and water's involvement in the binding and stabilization of thiamine (and its derivatives) to ShPrP to be analyzed, but it also led to the discovery of a slightly altered bound form compared to previously published results [3]. Our analysis of the inter-proton distances derived from our docking studies indicate that the restraints from experimental NOE data were reasonably well satisfied (Table 4). The majority of the distance deviations can be accounted for by spin diffusion artifacts resulting from the close proximity between thiamine's aminopyrimidine proton (H1') and Met138's alpha and Tyr150's aromatic protons [3]. In all of these protein–ligand complexes, the 4'-aminopyrimidine and thiazole rings occupy essentially the same region of conformational space within the binding site. The NOE restraints and calculated inter-proton distances are shown in Tables 3 and 4 for the V and F conformations, respectively.

Initially, in the docked V conformation, thiamine's 4-aminopyrimidine ring lies perpendicular to helix 1, with the amino group facing outside and the methyl group pointing towards the 4-hydroxyphenyl ring of Tyr150. The thiazole ring lies parallel to the plane of the imidazole group of His140. The OH and phosphate groups of thiamine and its derivatives point towards the amide nitrogen of Gly142. This orientation is very similar to the V conformation, where the C4–NH₂ group approaches the C2–H of the thiazolium [12, 13]. Several crystallographic studies observed this conformation for several thiamine-binding proteins [14, 15]. This may be due to steric interactions between C(2) and C(4') and subsequently those at C(4) and C(6'), which are the determining factors for these conformations. Generally, the docked

Table 3 Average inter-proton distances between docked thiamine and ShPrP in the V conformation. NOE restraints from 3LH8.pdb are given in parentheses

Ligand	Distance 1 (Å) Met138.H α –H1	Distance 2 (Å) Met139.H α –H1	Distance 3 (Å) His140.H β –H8	Distance 4 (Å) Gly142.HN–H12	Distance 5 (Å) Tyr150.H δ /H ϵ –H1
Thiamine	6.20 (2.70)	5.07 (5.0)	5.45 (2.70)	2.75 (2.70)	8.83 (2.70)
TMP	5.40 (2.70)	3.19 (5.0)	4.47 (2.70)	1.99 (2.70)	6.31 (2.70)
TDP	5.62 (2.70)	2.96 (5.0)	4.86 (2.70)	1.87 (2.70)	5.72 (2.70)
TPP	7.13 (2.70)	3.49 (5.0)	6.25 (2.70)	3.86 (2.70)	7.03 (2.70)

Table 4 Average inter-proton distances between docked thiamine and ShPrP in the F conformation. NOE restraints for 3LH8.pdb are given in parentheses

Ligand	Distance 1 (Å)		Distance 2 (Å)		Distance 3 (Å)		Distance 4 (Å)		Distance 5 (Å)	
	Met138.H α –H1		Met139.H α –H1		His140.H β –H8		Gly142.HN–H12		Tyr150.H δ /H ϵ –H1	
Thiamine	4.09	(2.70)	5.01	(5.0)	3.02	(2.70)	2.87	(2.70)	3.99	(2.70)
TMP	3.43	(2.70)	3.76	(5.0)	2.74	(2.70)	2.80	(2.70)	3.36	(2.70)
TDP	3.43	(2.70)	4.09	(5.0)	2.84	(2.70)	2.70	(2.70)	3.43	(2.70)
TPP	3.47	(2.70)	3.77	(5.0)	2.81	(2.70)	2.96	(2.70)	3.36	(2.70)

ligands displayed positive torsion angles for ϕ T and negative values for ϕ P. Similarly, these V torsion angles are observed for other thiamine-binding enzymes. For example, in yeast pyruvate decarboxylase (1PYD.pdb), yeast transketolase (1AY0.pdb), and thiamine phosphate synthase (IG4S.pdb) [16], N4 is positioned to deprotonate C2 of the thiazole ring. In these orientations, thiamine interacts with ShPrP through amino acids Asn143, Glu146, and Asp147. These orientations differ slightly from the previously reported structure, which shows the 4'-aminopyrimidine ring of thiamine perpendicular to the side chain of Tyr150 while forming an F conformation with positive torsion angles of ϕ T=3.5° and ϕ P=86.4°. In this F form, hydrogen-bonding interactions with negatively charged residues are absent.

Additional NOE-based restraint minimization of the thiamine-docked ShPrP resulted in slight structural changes of the protein. This new orientation, termed “protein II,” allowed π -stacking of Tyr150's side chain with the 4'-aminopyrimidine ring of thiamine. Subsequent blind docking of thiamine and its derivatives with this refined “protein II” structure placed the ligands in the pocket with an orientation similar to the conformation generated during restraint minimization [17]. The calculated distance between the aromatic protons of Tyr150 and the alpha proton of Met138 slightly exceeded the experimentally observed NOE restraints (Table 4).

Analysis of the X-ray structures for known thiamine-binding enzymes reveal that water frequently mediates the interactions between the ligand and the protein. For instance, water-mediated contacts between Gln154, Thr237, and Ser238 of thiamine phosphokinase and its thiamine ligand(s) are quite evident. Additionally, three water molecules bridge the interactions of Lys129, Tyr206, and Glu308 with the terminal phosphate group of TPP in the cancer-associated *Mycoplasma hyorhina* protein Mhp37. One water molecule bridges the interaction between Glu366, Thr388, and Gly340,

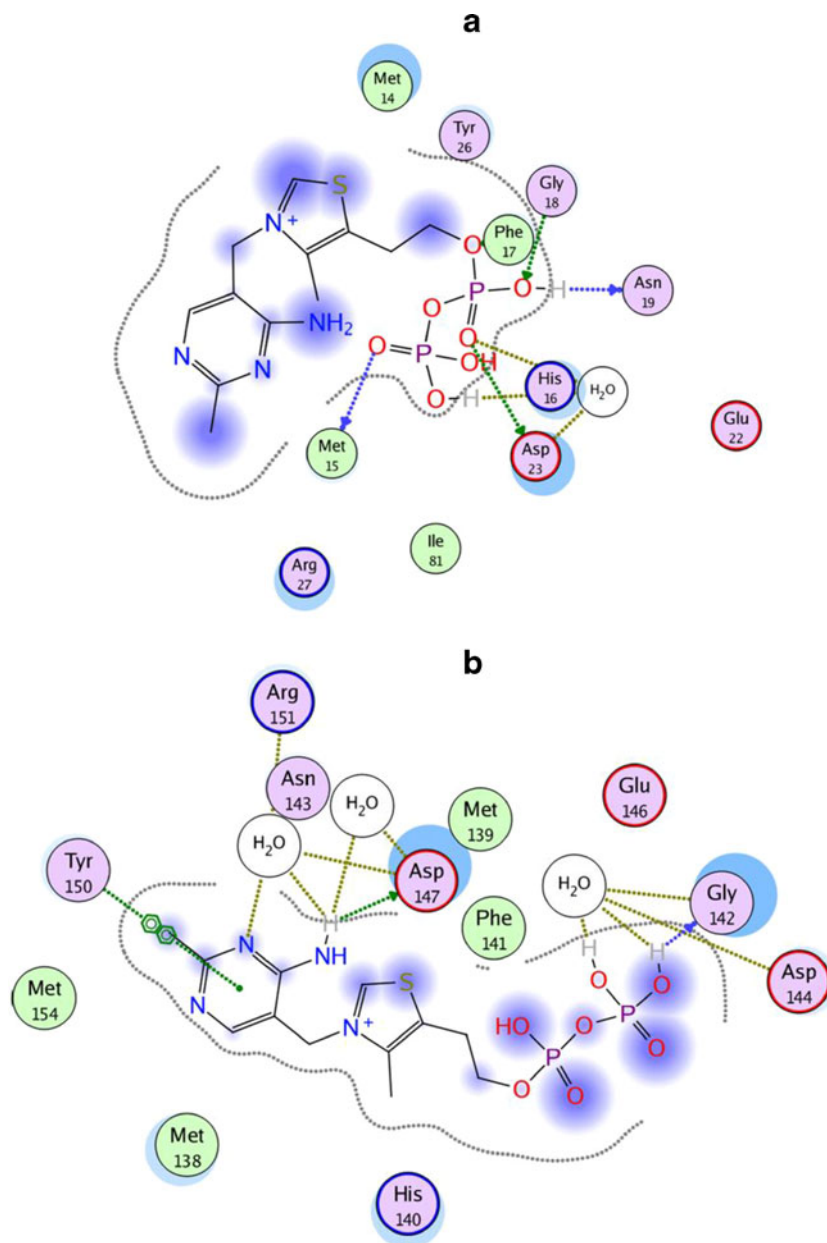
and another water molecule bridges the interaction between Asp155 and Asp185 in human transketolase. Finally, three water molecules form a bridge between the phosphate groups and Ser109, Asp230, and Lys258 in pyruvate dehydrogenase. For the prion protein, specifically when thiamine is in the V form, we found that dephosphorylated thiamine displays no interactions with water molecules, in contrast to what is seen for the other phosphorylated thiamine derivatives. For instance, TMP and TPP show interactions with three water molecules, while TDP shows interactions with only two water molecules. No water-bridging interactions between the ligand and protein are observed with these conformations. In our docking study, dephosphorylated thiamine binds via water-bridging hydrogen bonds between N1' and the side chain of Arg151. This interaction further stabilizes thiamine's pyrimidine ring electrostatically, with a calculated free energy of $-11.3 \text{ kcal/mol}^{-1}$. Two water molecules are involved in a network of interactions between the phosphate groups of TMP and TDP and side chains of Arg151 and Asp147. The total solvation free energies for these interactions are calculated to be $-7.9 \text{ kcal/mol}^{-1}$ and -9 kcal/mol^{-1} , respectively. Water also bridges the interaction between Asp147 and the 4'-amino group of the pyrimidine ring. In TPP binding, three water molecules are involved in a network of interactions with the phosphate and 4'-aminopyrimidine ring. One water molecule bridges the phosphate group with Gly142, and two water molecules bridge the N3 and N4 atoms of the 4'-aminopyrimidine ring to Asp147 and Arg151, respectively, with a solvation free energy of $-11 \text{ kcal/mol}^{-1}$.

Overall, the docking results for these enzymes and the prion protein indicate that our docking methodology is highly reliable, and that water-mediated interactions are important for the accurate prediction of thiamine–protein binding modes. This work demonstrates that water plays an important role in bridging thiamine-to-protein interactions, and that these

Table 5 Effect of mutations of the torsion angles (in degrees) for thiamine and its derivatives

Ligands	Initial V		Refined F		Y150A		Y150E		Y150L		Y150W		Y150F	
	ϕ T	ϕ P	ϕ T	ϕ P	ϕ T	ϕ P	ϕ T	ϕ P	ϕ T	ϕ P	ϕ T	ϕ P	ϕ T	ϕ P
Average	90	-18	32	62	67	-163	87	144	70	134	15	95	57	69
STD	34	110	11	16	6	4	10	18	37	29	51	18	7	14

Fig. 6a–b Interaction maps for the V (**a**) and F (**b**) conformations of TPP in the binding pocket of ShPrP



interactions are not easily resolved through NMR. Because water mediates many of the protein–ligand hydrogen bonds, including the interactions between the phosphate groups and the protein, they do not directly influence the binding constants, which were determined as $\sim 60 \mu\text{M}$ for all phosphorylated forms of thiamine.

Since Tyr150 plays an important role in stabilizing thiamine and its derivatives through π -stacking, *in silico* mutation studies (Tyr150Phe, Tyr150Trp, Tyr150Leu, Tyr150Glu, and Tyr150Ala) were carried out to investigate its role in mediating the binding between thiamine and the prion protein. Substituting Phe for Tyr150 had little effect on the binding orientation of thiamine. However, an effect on the orientation of the pyrimidine ring for the remaining mutants was observed

due to altered hydrophobicity and/or steric bulkiness of the residues. The Tyr150Ala mutant allowed for more room in the binding pocket, which oriented the 4'-aminopyrimidine ring into a conformation similar to the “S” conformation, with $\phi_T = \pm 100^\circ$ and $\phi_P = \pm 150^\circ$. The mutation Tyr150Glu allowed for electrostatic interactions between the acidic side chain of glutamic acid and thiamine’s pyrimidine ring. This was also seen with the S conformer (Table 5). The mutations Tyr150Phe, Tyr150Leu, and Tyr150Trp were used to evaluate the need for a hydrophobic interaction. Not surprisingly, when Tyr150 was mutated to Phe, a conformation similar to the initial docked thiamine resulted. The tryptophan mutant also allowed π -stacking in a classic F conformation; however, the bulkier side chain resulted in more deviation of the ϕ_T

dihedral angle (Table 5). For the leucine mutant, which maintains the hydrophobicity but lacks the ability to π -stack, similar results to those seen for the Y150E mutant were observed, whereby an S conformation was adopted along with larger deviations of both dihedral angles. Thus, from these results, we can conclude that π -stacking through the aromatic groups helps to mediate a consistent binding orientation of thiamine in an F conformation.

Conclusions

Molecular docking studies have provided further insights into and improved clarification of the common binding properties of thiamine with the prion protein. While these ligands adopt a V conformation with the prion protein during the initial docking phase, subsequent restraint minimization with NMR distances allows them to adopt an F conformation with the C2 carbon atom pointing over the pyrimidine ring. In this conformation, thiamine displayed π -stacking and water-mediated interactions. Based on these studies, we can conclude that the binding properties of thiamine and its derivatives are similar for both thiamine-dependent enzymes and for the prion protein.

Acknowledgments The authors wish to acknowledge the financial support of the Alberta Prion Research Institute (APRI), Alberta Innovates Bio-Solutions, the National Research Council of Canada (NRC-NINT), and the Canadian Institutes of Health Research (CIHR).

References

- Prusiner SB (1982) Novel proteinaceous infectious particles cause scrapie. *Science* 216:136–144
- Prusiner SB (1998) Prions. *Proc Natl Acad Sci USA* 95:13363–13383
- Perez-Pineiro R, Bjorndahl TC, Berjanskii MV, Hau D, Li L, Huang A, Lee R, Gibbs E, Ladner C, Dong YW, Abera A, Cashman NR, Wishart DS (2011) The prion protein binds thiamine. *FEBS J* 278:4002–4014
- Bjorndahl TC, Zhou GP, Liu XH, Perez-Pineiro R, Semenchenko V, Saleem F, Acharya S, Bujold A, Sobsey CA, Wishart DS (2011) Detailed biophysical characterization of the acid-Induced PrPc to PrP beta conversion process. *Biochemistry* 50:1162–1173
- Kuwata K, Nishida N, Matsumoto T, Kamatari YO, Hosokawa-Muto J, Kodama K, Nakamura HK, Kimura K, Kawasaki M, Takakura Y, Shirabe S, Takata J, Kataoka Y, Katamine S (2007) Hot spots in prion protein for pathogenic conversion. *Proc Natl Acad Sci USA* 104:11921–11926
- Timm DE, Liu JY, Baker LJ, Harris RA (2001) Crystal structure of thiamin pyrophosphokinase. *J Mol Biol* 310:195–204
- Sippel KH, Robbins AH, Reutzel R, Domsic J, Boehlein SK, Govindasamy L, Agbandje-McKenna M, Rosser CJ, McKenna R (2008) Structure determination of the cancer-associated *Mycoplasma hyorhinitis* protein Mh-p37. *Acta Crystallogr D* 64:1172–1178
- Nemeria NS, Arjunan P, Chandrasekhar K, Mossad M, Tittmann K, Furey W, Jordan F (2010) Communication between thiamin cofactors in the *Escherichia coli* pyruvate dehydrogenase complex E1 component active centers: evidence for a “direct pathway” between the 4'-aminopyrimidine N1' atoms. *J Biol Chem* 285:11197–11209
- Onufriev A, Bashford D, Case DA (2000) Modification of the generalized Born model suitable for macromolecules. *J Phys Chem B* 104:3712–3720
- Mackerell AD, Feig M, Brooks CL (2004) Extending the treatment of backbone energetics in protein force fields: limitations of gas-phase quantum mechanics in reproducing protein conformational distributions in molecular dynamics simulations. *J Comput Chem* 25:1400–1415
- Clark M, Cramer RD, Vanopdenbosch N (1989) Validation of the general-purpose Tripos 5.2 force-field. *J Comput Chem* 10:982–1012
- Pletcher J, Sax M (1972) Crystal and molecular structure of thiamine pyrophosphate hydrochloride. *J Am Chem Soc* 94:3998
- Lindqvist Y, Schneider G, Ermler U, Sundstrom M (1992) Three-dimensional structure of transketolase, a thiamine diphosphate dependent enzyme, at 2.5 Å resolution. *EMBO J* 11:2373–2379
- Muller YA, Schulz GE (1993) Structure of the thiamine and flavin-dependent enzyme pyruvate oxidase. *Science* 259:965–967
- Iwashima A, Nishimura H (1979) Isolation of a thiamine-binding protein from *Saccharomyces cerevisiae*. *Biochim Biophys Acta* 577:217–220
- Peapus DH, Chiu HJ, Campobasso N, Reddick JJ, Begley TP, Ealick SE (2001) Structural characterization of the enzyme-substrate, enzyme-intermediate, and enzyme-product complexes of thiamine phosphate synthase. *Biochemistry* 40:10103–10114
- Kern D, Kern G, Neef H, Tittmann K, Killenberg-Jabs M, Wikner C, Schneider G, Hubner G (1997) How thiamine diphosphate is activated in enzymes. *Science* 275:67–70